文章编号：1001－9014(2018)06－0699－06

DOI:10.11972/j.issn.1001－9014.2018.06.011

Optimization of growth temperatures for InAlAs metamorphic buffers and high indium InGaAs on InP substrate

ZHANG Jian[1,2], CHEN Xing-You[1], GU Yi[1*], Gong Qian[1], HUANG Wei-Guo[1,3], DU Ben[1,2], HUANG Hua[1], MA Ying-Jie[1], ZHANG Yong-Gang[1]

(1. State Key Laboratory of Functional Materials for Informatics, Shanghai Institute of Microsystem and Information Technology, Chinese Academy of Sciences, Shanghai 200050, China;
2. University of Chinese Academy of Sciences, Beijing 100049, China;
3. School of Physical Science and Technology, ShanghaiTech University, Shanghai 201210, China)

Abstract: $In_{0.83}Ga_{0.17}As$ layers were grown on InP substrate with InAlAs metamorphic buffers by gas source molecular beam epitaxy. The characteristics of InGaAs and InAlAs layers grown with different temperature schemes were investigated by high resolution X-ray diffraction reciprocal space maps, atomic force microscopy, photoluminescence and Hall-effect measurements. Results show that a higher growth temperature gradient of the InAlAs metamorphic buffers leads to a broader (004) reflection peak. The tilt angle between the epilayer and the substrate increases as well. The surface of the buffer layer becomes rougher. It indicates that the material defects increase and lattice relaxation becomes insufficient. $In_{0.83}Ga_{0.17}As$ layers were grown on the InAlAs metamorphic buffer with a fixed growth temperature gradient. A higher growth temperature leads to a moderate full width at half maximum along the Q_x direction of the (004) reflection, a stronger photoluminescence at 77 K, but a rougher surface of $In_{0.83}Ga_{0.17}As$. This indicates that the material defects can be suppressed at higher growth temperatures.

Key words: molecular beam epitaxy, InGaAs, InAlAs metamorphic buffer, growth temperature
PACS: 81.05.Ea, 81.15.Hi

InP衬底上InAlAs异变缓冲层和高铟组分InGaAs的生长温度优化

张 见[1,2], 陈星佑[1], 顾 溢[1*], 龚 谦[1], 黄卫国[1,3], 杜 奔[1,2], 黄 华[1], 马英杰[1], 张永刚[1]

(1. 中国科学院上海微系统与信息技术研究所 信息功能材料国家重点实验室, 上海 200050;
2. 中国科学院大学, 北京 100049;
3. 上海科技大学 物质科学与技术学院, 上海 201210)

摘要: 利用气态源分子束外延技术在InP衬底上生长了包含InAlAs异变缓冲层的$In_{0.83}Ga_{0.17}As$外延层. 使用不同生长温度方案生长的高铟InGaAs和InAlAs异变缓冲层的特性分别通过高分辨X射线衍射倒易空间图、原子力显微镜、光致发光和霍尔等测量手段进行了表征. 结果表明, InAlAs异变缓冲层的生长温度越低, X射线衍射倒易空间图(004)反射面沿Q_x方向的衍射峰半峰宽就越宽, 外延层和衬底之间的倾角就越大, 同时样品表面粗糙度越高. 这意味着材料的缺陷增加, 弛豫不充分. 对于生长在具有相同生长温度的InAlAs异变缓冲层上的$In_{0.83}Ga_{0.17}As$外延层, 采用较高的生长温度时, X射线衍射倒易空间图(004)反射面沿Q_x方向的衍射峰半峰宽较小, 77 K下有更强的光致发光, 但是表面粗糙度会有所增加. 这说明生长温度提高后, 材料中的缺陷得到抑制.

关 键 词: 分子束外延; InGaAs; InAlAs异变缓冲层; 生长温度
中图分类号: TN215　　**文献标识码**: A

Received date: 2018-02-03, **revised date**: 2018-08-24　　**收稿日期**: 2018-02-03, **修回日期**: 2018-08-24
Foundation items: Supported by the National Key Research and Development Program of China (2016YFB0402400), National Natural Science Foundation of China (61775228, 61675225, and 61605232), and the Shanghai Rising-Star Program (17QA1404900)
Biography: ZHANG Jian(1990-), male, Zoucheng, China. Ph. D. Research fields focus on material and device of Ⅲ/Ⅴ compound semiconductors. E-mail: jianzhang@mail.sim.ac.cn
* **Corresponding author**: E-mail: ygu@mail.sim.ac.cn

Introduction

The ternary III-V compound semiconductor, $In_xGa_{1-x}As$ ($0 \leqslant x \leqslant 1$), with the band gap ranging from 0.35 to 1.42 eV, has significant applications for optoelectronic devices in the infrared area, such as light emitters, thermophotovoltaics, and photodetectors etc.[1-4] In recent years, there is a great demand for infrared detectors with the cutoff wavelength range of 1 ~ 3 μm, in the applications of spectroscopy and space imaging, including the earth observation, the remote sensing, and the environmental monitoring, etc.[5] However, with the response wavelength extended to longer than 1.7 μm, the increasing lattice mismatch between the $In_xGa_{1-x}As$ ($0.53 \leqslant x \leqslant 1$) and the InP substrate will result in poorer material quality with respect to $In_{0.53}Ga_{0.47}As$. In order to overcome this limitation, the $In_xAl_{1-x}As$ (referred to as InAlAs hereafter) metamorphic buffer layer has been introduced to alleviate the impact of lattice mismatch and accommodate the strain in the high indium (In) InGaAs layer.

The growth temperature is one of the most basic parameters for the growth technique of molecular beam epitaxy (MBE). Generally, a low growth temperature may incorporate background impurities into the epilayers during the growth process. Whereas an over high growth temperature may enhance the In segregation on the surface especially for InGaAs with a high In content[6], which will cause poor surface morphology and composition non-uniformity in the epilayer. In previous, the growth temperature of high In InGaAs detector was optimized in a relatively limited range[7]. To acquire higher quality InGaAs with high In content on InP, the growth temperatures of both InGaAs and InAlAs metamorphic buffer layers should be optimized.

In this paper, we focused on the effects of the growth temperature schemes on the crystal quality of both the InAlAs metamorphic buffer and the high In InGaAs layers[8]. Firstly, for the growth of 2 μm thick InAlAs metamorphic buffer layers, three different growth temperature gradients of 20, 30 and 40℃/μm were studied. Secondly, for the growth of $In_{0.83}Ga_{0.17}As$ layers on the InAlAs metamorphic buffer with the growth temperature gradient fixed at 20℃/μm, three different growth temperature schemes of 545℃, 530℃ and 515℃ were studied. Results show that the structural, optical and electrical properties vary with the growth temperature.

1 Experiments

Samples in this study were grown on (001)-oriented semi-insulating InP epi-ready substrates by using a VG Semicon V80H GSMBE system. For the growth, arsenic (AsH_3) and phosphorus (PH_3) cracking cells were equipped as group V sources. Their fluxes were controlled by adjusting the pressure and the cracking temperature was around 1 000℃. Other sources were all elemental solid; gallium (Ga), In and aluminum (Al) were used as group III sources, and their fluxes were controlled by changing the temperature of cells. The temperatures of different sources were monitored by respective thermocouples. The surface oxide of the substrate was desorbed under the P_2 flux at around 590℃ and this desorption process was monitored by a reflection high energy electron diffraction. During growth, the pressure of the growth chamber was kept typically on the level of 10^{-5} Torr.

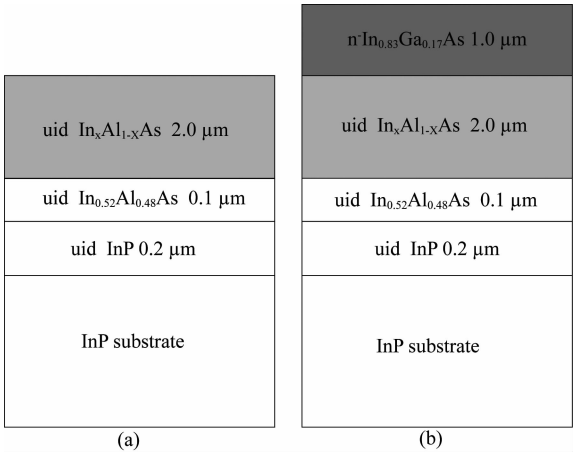

Fig. 1 Structures of the InAlAs metamorphic buffer layer and $In_{0.83}Ga_{0.17}As$ grown at different temperatures

图 1 不同温度下生长的 InAlAs 异变缓冲层和 $In_{0.83}Ga_{0.17}As$ 的结构图

Table 1 Growth parameters and results for InAlAs metamorphic buffer layers grown at different temperatures

表 1 不同温度下生长的 InAlAs 异变缓冲层生长参数和测试结果

Sample	Growth temperature /℃	Temperature gradient/(℃/ m)	FWHM of (004) (1×10^4 rlu)	RMS/nm
A1	540→500	20	35	2.2
A2	540→480	30	43	3.4
A3	540→460	40	46	3.6

As increasing the In content in the $In_xAl_{1-x}As$ metamorphic buffer layers, the growth temperature was reversely graded, where three temperature gradients were adopted. As shown in Fig. 1(a), the structure of the first group of InAlAs samples consisted of a 0.2 μm-thick InP buffer layer, a 0.1 μm-thick $In_{0.52}Al_{0.48}As$ matching layer, and a 2-μm-thick $In_xAl_{1-x}As$ continuously graded buffer layer. All the epilayers were unintentionally doped. With the In composition in the InAlAs buffer layers graded from 0.52 to 0.86, the growth temperatures decreased from 540℃ to 500, 480 and 460℃, corresponding to the decreasing rates of 0.006, 0.009, 0.012℃/s and temperature gradients of 20, 30 and 40℃/μm, and these samples were named as samples A_1, A_2 and A_3, respectively. For the growth of $In_{0.83}Ga_{0.17}As$ in the second group, a 1-μm-thick $In_{0.83}Ga_{0.17}As$ layer was grown on the InAlAs metamorphic buffer with the temperature gradient fixed at 2℃/μm. The growth temperatures were 545, 530 and 515℃, and these samples were named as samples B_1, B_2 and B_3, re-

spectively.

After growth, a Bruker Dimension-Icon atomic force microscope (AFM) was used to characterize the surface of the samples. High resolution X-ray diffraction (HRXRD) reciprocal space mapping (RSM) measurements were performed in a Philips X'pert materials research diffractometer with a four-crystal Ge (220) monochromator. The photoluminescence (PL) spectra were measured by using a Thermo Scientific Nicolet iS50 Fourier transform infrared (FTIR) spectrometer equipped with a liquid-nitrogen cooled InSb detector and a CaF_2 beam splitter; in addition, a diode-pumped solid-state (DPSS) laser with the wavelength of 532 nm was used as the excitation source. The carrier concentration and mobility of the samples were characterized by a Hall-effect measurement system.

2 Results and discussions

(1) InAlAs metamorphic buffer layers grown at different temperature gradients

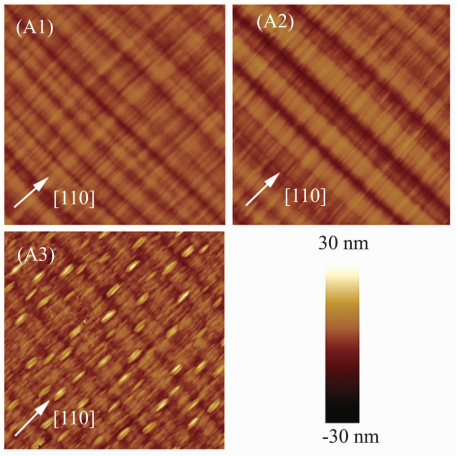

Fig. 2　AFM images of the InAlAs metamorphic buffer layers grown at different temperature gradients. The AFM image sizes are 20 μm × 20 μm for all three samples
图 2　不同温度梯度下生长的 InAlAs 异质缓冲层样品的 AFM 图像,扫描范围均为 20 μm × 20 μm

Figure 2 shows the 20 μm × 20 μm AFM images of the InAlAs metamorphic buffer layers grown at different temperature gradients. Clear cross-hatch morphology can be seen on all sample surfaces under the low magnification, which is the typical surface morphology of metamorphic epi-structures[9]. This cross-hatch morphology is usually observed in the lattice-mismatched III-V semiconductor heterostructures with zinc-blende structures and stemmed from the two types of misfit dislocations (MDs) lying along the [1-10] and [110] directions, presumably with group V and group III atom-based cores, respectively[10]. From Fig. 2, we can see that the primary ridges of those three samples are parallel along the [1-10] direction, and the oval-like undulations pop on the top of the primary ridges, causing the secondary ridges and valleys with smaller periods along the [110] direction. The cross-hatch pattern mimics the network of misfit dislocations underneath. The MDs cause strain non-uniformity at the growth front, which induces preferential deposition of the Al and In atoms and thus thickness and alloy fluctuations. The roughness of the samples resulted from the cross-hatch in a large scale is superimposed by other three-dimensional (3D) features such as dots and mounds in a small scale. The root-mean-square (RMS) roughness values of samples A_1, A_2 and A_3 are 2.2, 3.4 and 3.6 nm, respectively. It can be deduced that with the increase of the growth temperature gradient, the roughness of the sample surface gradually increases.

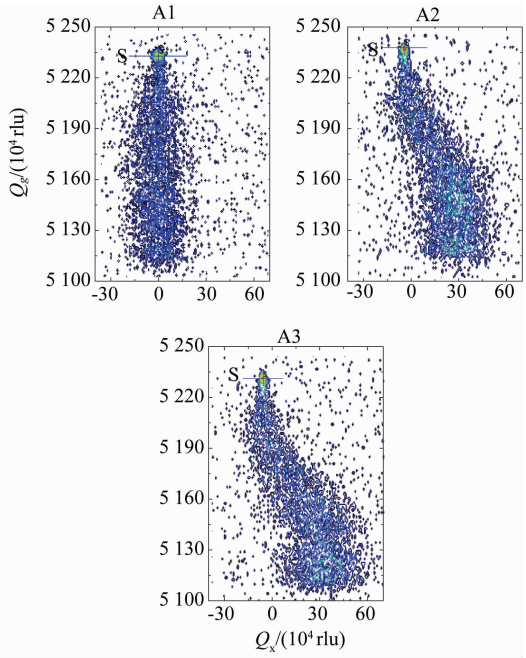

Fig. 3　HRXRD RSM images of the InAlAs metamorphic buffer layer on InP substrate for (004) reflection
图 3　InP 上生长的 InAlAs 异变缓冲层(004)面的 XRD 倒易空间衍射图

Comprehensive lattice characteristics of the metamorphic structures can be achieved by HRXRD RSM measurements, including the lattice tilting, the relaxation status and the compositions. Figure 3 shows the RSMs of the InAlAs metamorphic buffer layers grown at different temperature gradients. In all the RSM images, the intensities are in the logarithmic scale. The narrow and circular peaks correspond to the InP substrate, and the gradually widening patterns from the substrate to the upper layer are observed, corresponding to the compositionally graded InAlAs buffer. Generally, the diffuse scatterings on the normal lines are due to the composition fluctuation in the layer, and the diffuse scatterings perpendicular to the normal lines are mainly related to the dislocations[11]. Figure 3 quantitatively plots the (004) reflections of the InAlAs buffer layers for the three samples. From the RSM images, we can see that the full width at half maximums (FWHMs) along the Q_x direction in RSMs of samples A_1, A_2 and A_3 are around 3.5×10^5, 4.3×10^5, and 4.6×10^5 rlu, respectively. As the growth temperature gradient increases, the FWHM of the epitaxial layer gradually increases, which means that the

dislocation density in the epitaxial layer gradually became larger. Moreover, the tilt angle between the substrate and the epitaxial layer in the (004) reflection of RSM image is also different. It is observed that the tilt angle of all three samples is 0.05°, 0.40° and 0.43°, respectively. It indicates that as the sample growth temperature becomes lower, the tilt angle increased dramatically. The variation trend of RSM FWHMs is in good agreement with the AFM results.

(2) $In_{0.83}Ga_{0.17}As$ grown at different temperatures

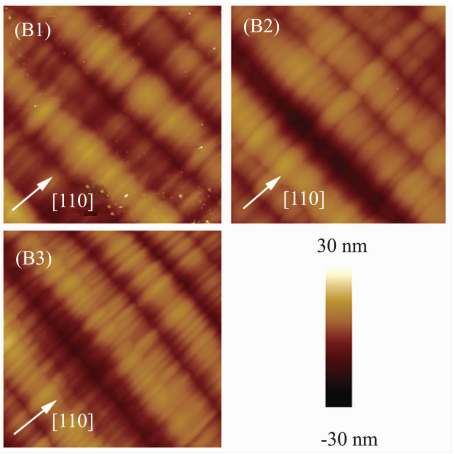

Fig. 4 AFM images of the $In_{0.83}Ga_{0.17}As$ grown at different temperatures. The AFM image sizes are 20 μm × 20 μm for all three samples

图4 不同温度下生长的 $In_{0.83}Ga_{0.17}As$ 样品的 AFM 图像,扫描范围均为 20 μm × 20 μm

Figure 4 shows the typical AFM images of the $In_{0.83}Ga_{0.17}As$ grown at different temperatures. The normal cross-hatch morphology is also shown in all three samples. The skeleton of the cross-hatch pattern is similar with that observed in the InAlAs metamorphic buffer layers grown at different temperature gradients, but the oval-like defects seems more distinct, and the undulations of the patterns along the [110] and [1-10] directions are larger than those of InAlAs buffers. This indicates that the misfit strain is relaxed more thoroughly with thickening the epilayer by introducing MDs. The RMS roughness values of 6.1, 5.6, and 5.2 nm are observed for samples B_1, B_2, and B_3, respectively. It is clear that with the gradual decrease of the growth temperature, the roughness of the sample surface gradually decreases.

Figure 5 shows the (004) and (115) reflection RSMs of the $In_{0.83}Ga_{0.17}As$ grown at different temperatures. The narrow and circular peaks correspond to the InP substrate while the elliptical peaks correspond to the metamorphic $In_{0.83}Ga_{0.17}As$ layer with a larger diffuse scattering perpendicular to the normal line. Between the InP substrate and the $In_{0.83}Ga_{0.17}As$ layer, gradually widening patterns from the substrate to the upper layers are also observed, corresponding to the compositionally graded $In_xAl_{1-x}As$ buffer. It is observed that the FWHMs along the Q_x direction of the (004) reflection of samples B_1, B_2, and B_3 are around 4.2×10^5 rlu, 6.9×10^5 rlu,

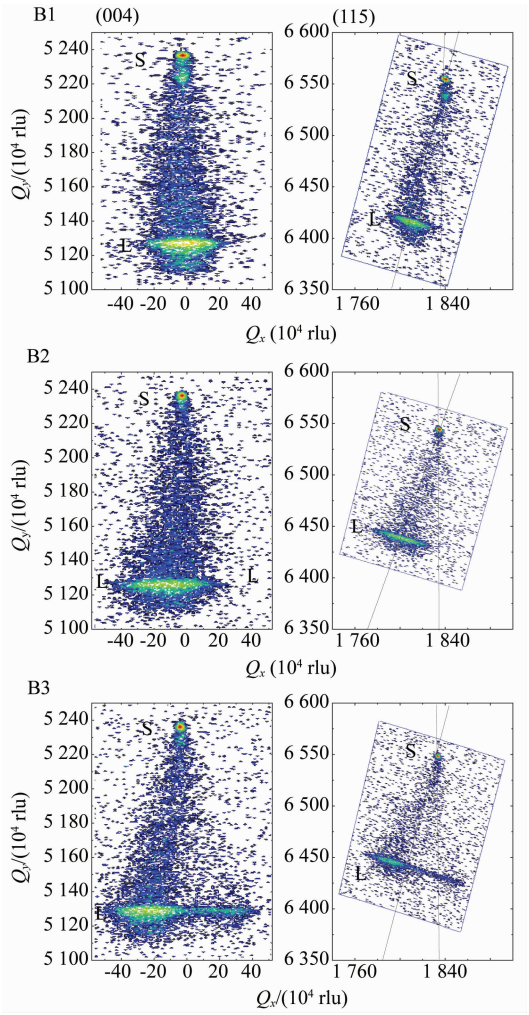

Fig. 5 HRXRD RSM images of the $In_{0.83}Ga_{0.17}As$ layer on the InP substrate for the (004) and (115) reflections

图5 InP 上生长的 $In_{0.83}Ga_{0.17}As$ 外延层(004)和(115)面的 XRD 倒易空间衍射图

and 1.2×10^6 rlu, respectively. The FWHM along the Q_x direction of (004) reflection gradually increases as the growth temperature decreases. It indicates that the defects in the material gradually increase as the growth temperature decreases.

The PL measurement is an essential method to reveal the optical quality of the epi-layer. Figure 6 shows the PL spectra of the $In_{0.83}Ga_{0.17}As$ layers at 77 K. The PL peaks centered at about 0.523 eV correspond to the $In_{0.83}Ga_{0.17}As$ layer. It is noticed that the valley located at 0.522 eV is caused by the absorption of H-O radical in the SiO_2 window mounted on the helium-cooled cryostat. With the increase of the growth temperature, the PL intensity of $In_{0.83}Ga_{0.17}As$ increases correspondingly. This indicates that as the growth temperature of the $In_{0.83}Ga_{0.17}As$ layer increases, the number of non-radiative recombination centers is decreased.

The unintentionally doped $In_{0.52}Al_{0.48}As$ or InAlAs metamorphic buffer layers show a high resistive feature[12]. The contribution of the buffer structure under-

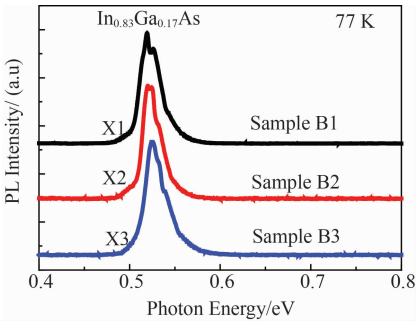

Fig. 6　The PL spectra of the $In_{0.83}Ga_{0.17}As$ grown at different temperatures measured at 77 K

图 6　在 77 K 测得的不同温度生长的 $In_{0.83}Ga_{0.17}As$ 样品的 PL 光谱

neath the $In_{0.83}Ga_{0.17}As$ layer to the electrical properties can be negligible. Table 2 shows the room temperature (RT) and 77 K carrier mobility of the $In_{0.83}Ga_{0.17}As$ grown at different temperatures. At first, the RT carrier mobility decreases slightly from 1.03×10^4 to 9.42×10^3 cm^2/Vs when the growth temperature of $In_{0.83}Ga_{0.17}As$ increases from 515 to 530℃, and then the carrier mobility decreases slightly to 9.40×10^3 cm^2/Vs when the growth temperature of $In_{0.83}Ga_{0.17}As$ is increased to 545℃. At RT, the carrier concentration of samples B_1, B_2 and B_3 is about $4.0 \times 10^{16}/cm^3$. By cooling the samples down to 77 K, the carrier mobility decreases from 2.70×10^4 to 2.50×10^4 cm^2/Vs when the growth temperature of $In_{0.83}Ga_{0.17}As$ is increased from 515 to 530℃, and then the carrier mobility decreases to 2.31×10^4 cm^2/Vs for sample B_1 grown at 545℃. At 77 K, the carrier concentration of samples B_1, B_2 and B_3 is about $3.0 \times 10^{16}/cm^3$. Although the variations of the Hall mobility among the three samples are limited, the paralleled comparison between the three samples is still feasible as the measurement process is carefully kept the same for the three samples. It has been reported that several carrier scattering mechanisms dominating in different temperature ranges coexist in lattice-matched $In_{0.53}Ga_{0.47}As$ and lightly lattice-mismatched $_xGa_{1-x}As$ alloys[13-14]. As shows in the AFM results, the surface roughness of the $In_{0.83}Ga_{0.17}As$ material increases as the growth temperature increased. Therefore, we infer that due to the higher roughness of the interface, the disorder scattering mechanism of the alloy may increase at higher growth temperatures.

3　Conclusions

In order to study the effect of different growth temperatures on the crystal quality, the characteristics of two sets of samples grown in different temperature schemes were investigated. AFM shows that a relatively lower growth temperature is beneficial for the smoothness of the $In_{0.83}Ga_{0.17}As$ surface, while causes a rougher surface of the composition continuously graded InAlAs buffer layer. A higher growth temperature can enhance the PL intensity of $In_{0.83}Ga_{0.17}As$ layer by eliminating the non-radiative recombination centers in the material. However, a higher growth temperature leads to a slight decrease in carrier mobility.

References

[1] Nagai H, Noguchi Y. Crack formation in InP-$Ga_xIn_{1-x}As$-InP double-heterostructure fabrication [J]. *Applied Physics Letters*, 1976, **29**(11): 740-741.

[2] Bandy S, Nishimoto C, Hyder S, *et al*. Saturation velocity determination for $In_{0.53}Ga_{0.17}As$ field-effect transistors [J]. *Applied Physics Letters*, 1981, **38**(10): 817-819.

[3] Murray S L, Newman F D, Murray C S, *et al*. MOCVD growth of lattice-matched and mismatched InGaAs materials for thermophotovoltaic energy conversion [J]. *Semiconductor Science and Technology*, 2003, **18**(5): s202-s208.

[4] Bachmann K J, Shay J L. An InGaAs detector for the 1.0-1.7 μm wavelength range [J]. *Applied Physics Letters*, 1978, **32**(7): 446-448.

[5] Hoogeveen R W M, Vander A R J, Goede A P H. Extended wavelength InGaAs infrared (1.0-2.4 μm) detector arrays on SCIAMACHY for space-based spectrometry of the Earth atmosphere [J]. *Infrared Physics and Technology*, 2001, **42**(1): 1-16.

[6] Toikkanen L, Hakkarainen T, Schramm A, *et al*. Metamorphic growth of tensile strained GaInP on GaAs substrate [J]. *Journal of Crystal Growth*, 2010, **312**(21): 3105-3110.

[7] Gu Y, Zhang Y G, Wang K, *et al*. Effects of growth temperature and buffer scheme on characteristics of InP-based metamorphic InGaAs photodetectors [J]. *Journal of Crystal Growth*, 2013, **378**: 65-68.

[8] Globisch B, Dietz R J B, Stanze D, *et al*. Carrier dynamics in Beryllium doped low-temperature-grown InGaAs/InAlAs [J]. *Applied Physics Letters*, 2014, **104**(17): 1-4.

[9] Shiryaev S Y, Jensen F, Petersen J W. On the nature of cross-hatch patterns on compositionally graded Si_xGe_{1-x} alloy layers [J]. *Applied Physics Letters*, 1994, **64**(24): 3305-3307.

[10] Hudait M K, Lin Y, Wilt D M, *et al*. High-quality $InAs_yP_{1-y}$ step-graded buffer by molecular-beam epitaxy [J]. *Applied Physics Letters*, 2003, **83**(3): 587-587.

[11] Fewster P F. X-ray diffraction from low-dimensional structures [J]. *Semiconductor Science and Technology*, 1993, **8**(11): 1915-1934.

Table 2　Growth parameters and results for $In_{0.83}Ga_{0.17}As$ grown at different temperatures

表 2　不同温度生长的 $In_{0.83}Ga_{0.17}As$ 的生长参数和测试结果

Sample	Growth temperature/℃		Relaxation degree /(%)	$FWHM_x$ of (004) (1×10^4 rlu)	RMS/nm	Hall Mobility /($cm^2 V^{-1} s^{-1}$)	
	InAlAs	$In_{0.83}Ga_{0.17}As$				RT	77 K
B1	540→500	545	92.2	42	6.1	9.40×10^3	2.31×10^4
B2	540→500	530	94.2	69	5.6	9.42×10^3	2.50×10^4
B3	540→500	515	88.2	120	5.2	1.03×10^4	2.70×10^4

(下转第 710 页)